Available online at www.sciencedirect.com
ScienceDirect
Progress in Natural Science 19 (2009) 461–470
Progress in Natural Science
www.elsevier.com/locate/pnsc

Evaluation of earthquake-induced structural damages by wavelet transform

Hongnan Li [a], Tinghua Yi [a,b,*], Ming Gu [b], Linsheng Huo [a]

[a] *State Key Laboratory of Coastal and Offshore Engineering, Dalian University of Technology, School of Civil and Hydraulic Engineering, No. 2 Linggong Road, Ganjingzi District, Dalian, Liaoning Province 116024, China*
[b] *State Key Laboratory for Disaster Reduction in Civil Engineering, Tongji University, Shanghai 200092, China*

Received 28 April 2008; received in revised form 17 July 2008; accepted 9 September 2008

Abstract

The dynamic behavior of inelastic structures during an earthquake is a complicated non-stationary process that is affected by the random characteristics of seismic ground motions. The conventional Fourier analysis describes the feature of a dynamic process by decomposing the signal into infinitely long sine and cosine series, which loses all time-located information. However, both time and frequency localizations are necessary for the analysis of an evolutionary spectrum of non-stationary processes. In this paper, an analytical approach for seismic ground motions is developed by applying the wavelet transform, which focuses on the energy input to the structure. The procedure of identification of the instantaneous modal parameters based on the continuous wavelet transform (CWT) is given in detail. And then, a novel method using the auto-regressive moving average (ARMA), called "prediction extension", is presented to remedy the edge effect during the numerical computation of the CWT. The effectiveness of the method is verified by the use of the benchmark model developed by the American Society of Civil Engineers (ASCE). Finally, a scale model with three-storey reinforced concrete frame-share wall structure is made and tested on a shaking table to investigate the relation between the dynamic properties of structures and energy accumulation and its change rates during the earthquake. The results have shown that the wavelet transform is able to provide a deep insight into the identity of transient signals through time-frequency maps of the time variant spectral decomposition.
© 2008 National Natural Science Foundation of China and Chinese Academy of Sciences. Published by Elsevier Limited and Science in China Press. All rights reserved.

Keywords: Earthquake; Structural damage; Wavelet transform; Frame-share wall structure

1. Introduction

The rapid development of the global urban landscape continues to propel buildings to new heights and spans, enhancing the role of structural engineers in assuring a safe and habitable built environment [1]. Among all the natural disasters, the earthquake is one of the most serious ones. It brings tremendous economic losses and deaths of people, as well as the enormous effects on the harmonious and continuous development of society. For example, there were earthquake disasters in Los Angeles, USA, in 1994 (61 fatalities and 40 billion US dollars in losses); Kobe, Japan, in 1995 (over 6400 fatalities and 100 billion US dollars in losses); Kocaeli, Turkey, in 1999 (over 15,000 fatalities and 20 billion US dollars in losses); Athens, Greece, in 1999 (143 fatalities and 2 billion US dollars in losses); Taiwan, China in 1999 (over 2300 fatalities and 9 billion US dollars in losses) [2]; and Wenchuan, China in 2008. The collapse and failure of these deficient structures caused increasing concern for the structural integrity, durability and reliability. An earthquake usually leads to stiffness and strength deterioration of a structure at a global level. When the visual inspection of structural elements in a building is unfeasible or the appearance of damage is not obvious, estimating and correlating such degradations with

* Corresponding author. Tel./fax: +86 411 84706050.
E-mail address: yth@dlut.edu.cn (T. Yi).

1002-0071/$ - see front matter © 2008 National Natural Science Foundation of China and Chinese Academy of Sciences. Published by Elsevier Limited and Science in China Press. All rights reserved.
doi:10.1016/j.pnsc.2008.09.002

?1994-2018 China Academic Journal Electronic Publishing House. All rights reserved. http://www.cnki.net

meaningful and descriptive damage assessment (e.g. safe, lightly damaged, damaged, critically damaged) forms the basis for making suitable repair decisions on the damaged structure. In such cases, the time histories of recorded excitation and response during the earthquake event are usually used for reliable post-earthquake estimation of local and global damage in the structure [3–6].

It is well known that the dynamic behavior of an inelastic structure during an earthquake is a complex non-stationary process that is affected by the random characteristics of ground motions not only in the frequency domain but also in the time domain. Thus, the structural safety under the earthquake cannot be estimated by the energy spectra that are only defined in the frequency domain. For example, the Hachinohe motions recorded during the Tokachi-Oki earthquake in 1968 and the JMA-Kobe motions recorded during the Hyogoken-Nanbu earthquake in 1995, which are of oceanic type and epicentral type, respectively, have the same Fourier amplitudes; in other words, the same total energy inputs at the vicinity of the 1.0 s period. But they exhibited a considerable difference in destructiveness to the structures with a 1.0-s natural period in such a way that the epicentral motions having a larger rate of energy input in the time domain can knock down the structures more devastatingly than the oceanic type motions [7]. As the inability of the conventional Fourier analysis preserves the time dependence, new analytical methods are required to describe the evolutionary spectral characteristics of non-stationary processes in both frequency and time domains. Among the most commonly used time-frequency methods are the Wigner-Ville and Gabor representations. Yet, these approaches also suffer from several drawbacks. The Wigner-Ville transform shows spurious interference phenomena due to the quadratic form of the transformation [8]. The Gabor transform, although taking advantage of optimal time-frequency localization according to Heisenberg's uncertainty principle, suffers from the drawback of having fixed windows; a disadvantage common to all windowed Fourier transforms [9].

The wavelet transform is a new method to analyze signals, which overcomes the problems that other signal processing techniques exhibit. The main advantage gained by using the wavelet transform is the ability to perform the local analysis of a signal, i.e. to zoom in any interval of time or space. Wavelet analysis is thus capable of revealing some hidden aspects of the data that other signal analysis techniques fail to detect. Thereby, this property is particularly important for damage detection of structures. Moreover, due to the availability of a fast transform version, the computational effort to perform the signal transformation is reduced. Because of these features, the wavelet transform is proposed as a promising new method for damage identification in structures. This paper presents an analytical method of seismic ground motions focusing on the energy input to structures, which can transform the sequential data in a time domain such as earthquake acceleration records to the spectral data in both time and frequency domains with the adaptive windows. Moreover, it describes the application of the CWT method to frequency-modulated signals with a description of the general theoretical background; and proposes a new method to overcome the problem posed by the edge effect.

2. Theoretical background of wavelet transforms

In a nutshell, the wavelets are the localized waves with a zero average value that drops to zero after a few oscillations. General reviews of wavelet theory may be referred to Chui [10] and Daubechies [11]. The wavelet transform includes the continuous wavelet transform (CWT) and discrete wavelet transform (DWT). The main advantage of the CWT is its ability to provide the information simultaneously in time and scale with adaptive windows. The CWT offers promising tools for the estimation of modal parameters and new perspectives for damage identification of the structures. Two main features make the CWT particularly attractive. Firstly, the vibration modes can be automatically decoupled in most cases where the natural frequencies are not too close, which allows for an accurate extraction of the instantaneous frequencies and damping parameters. Secondly, the essential information is contained in a small subset of the CWT, namely in the maxima lines and ridges.

Suppose that the function $x(t)$ satisfies the following condition:

$$\int_{-\infty}^{\infty} |x(t)|^2 \, \mathrm{d}t < \infty \tag{1}$$

which implies that $x(t)$ decays to zero at $\pm\infty$. Then, the CWT can be defined as

$$W(a,t) = \frac{1}{\sqrt{a}} \int_{-\infty}^{+\infty} x(\tau) g * \left(\frac{\tau - t}{a}\right) \mathrm{d}t \tag{2}$$

where $*$ denotes the complex conjugate. The dilation by the scale, a, inversely proportional to the frequency, represents the periodic or harmonic nature of the signal. The resulting wavelet coefficient, $W(a,t)$, means a measurement of the similitude between the dilated/shifted parent wavelet and the signal at time t and scale (frequency) a. The normalization by the root of scale insures that the integral energy given by the wavelet is independent of the dilation. These observations describe the multi-resolution property of the wavelet transform (see Fig. 1).

The function $g(t)$ qualifies for analyzing the wavelet when it satisfies the admissibility condition:

$$C_g = \int_{-\infty}^{+\infty} \frac{|G(f)|^2}{|f|} \, \mathrm{d}f < \infty \tag{3}$$

where $G(f)$ is the Fourier transform of $g(t)$. This is necessary for obtaining the inverse of the wavelet transform given by

$$x(t) = \frac{1}{C_g} \int_{-\infty}^{+\infty} \int_{-\infty}^{+\infty} W(a,t) \frac{1}{\sqrt{a}} g^* \left(\frac{t - \tau}{a}\right) \frac{\mathrm{d}a \, \mathrm{d}\tau}{a^2} \tag{4}$$

?1994-2018 China Academic Journal Electronic Publishing House. All rights reserved. http://www.cnki.net

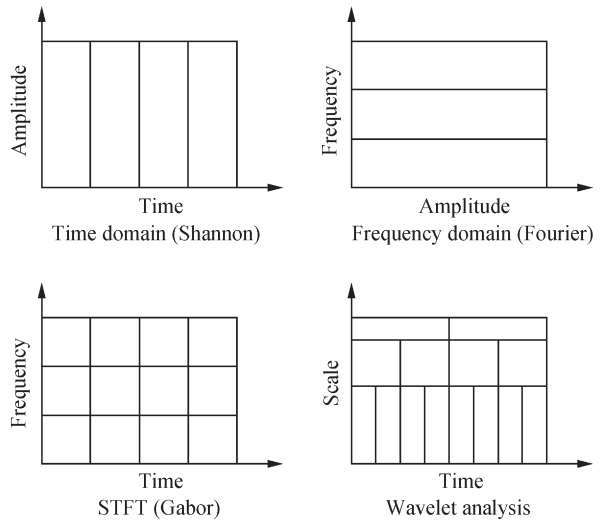

Fig. 1. Comparison of four different transformations.

The time-frequency localization derived from $g(t)$ may be a window function, which additionally means

$$\int_{-\infty}^{\infty} |g(t)|t < \infty \tag{5}$$

In practice, some regularity and smoothness on the wavelet function are also required.

The calculation of the wavelet transform can be expedited in the frequency domain through the use of the Fourier transforms. Thus, the convolution in Eq. (2) can equivalently be represented as a product in the Fourier domain with Fourier frequency, f,

$$W(a,t) = \sqrt{a}\int_{-\infty}^{\infty} \widehat{X}(f)\widehat{G}^*(af)e^{i2\pi ft}\,\mathrm{d}f \tag{6}$$

where $\widehat{X}$ and $\widehat{G}$ are the Fourier transform of the signal and the parent wavelet, respectively.

There are a number of different complex- and real-valued functions that are used as analyzing wavelets [12]. In many cases, the so-called progressive wavelet function is used, which is a complex-valued function that satisfies the admissibility condition and does not have any negative frequencies. One of the most widely used functions in the wavelet analysis is the Morlet wavelet defined by

$$g(t) = e^{i\omega_0 t} - e^{-t^2/2} \tag{7}$$

Essentially, the Morlet wavelet in Eq. (7) is a Gaussian-windowed Fourier transform with sines and cosines oscillation at the central frequency, f_0 ($\omega_0 = 2\pi f_0$). The Morlet wavelet is equivalently localized in the frequency domain, as evidenced by the Fourier transform of the dilated Morlet wavelet

$$G(af) = \sqrt{2}\sqrt{\pi}e^{-2\pi^2}(af - f_0)^2 \tag{8}$$

For the Morlet wavelet, there is a unique relationship between the dilation parameter of the transform, a, and the Fourier frequency, f, on which the wavelet is focused. This relationship is evident by maximizing Eq. (8) to yield

$$a = f_0/f \tag{9}$$

3. Wavelet modal extraction technique

3.1. Ridges and skeletons of wavelet transform

The wavelet-based system identification from the impulse response function and free vibration response is made on the development of the complex analytical signal, taking the form of an exponential function given by

$$z(t) = A(t)e^{i\phi(t)} \tag{10}$$

where $A(t)$ and $\phi(t)$ are the time-varying amplitude and phase, respectively. Therefore, the concept of instantaneous frequency as the time-varying derivative of the phase is

$$f(t) = \frac{1}{2\pi}\frac{\mathrm{d}}{\mathrm{d}t}\phi(t) \tag{11}$$

Thus, the phase of the complex-valued analytical function provides a simple method to identify the time-varying frequency of the system. In the case of free vibration decaying curves, the oscillator responds at the damped natural frequency ω_D, and the time-varying amplitude term takes the form of an exponential, decaying based on the system natural frequency $\omega_n = 2\pi f_n$ and damping ξ ($\omega_D \approx \omega_n$, for lightly damped systems):

$$z(t) = (A_0 e^{-\xi\omega_n t})e^{i(\omega_D t+\theta)} \tag{12}$$

where A_0 is the initial amplitude value and θ denotes the phase shift. Note that this complex analytical signal would typically be generated by

$$z(t) = x(t) + iH[x(t)] \tag{13}$$

where $x(t)$ means the original signal and $H[\cdot]$ represents the Hilbert transform.

The square of the modulus of the wavelet transform can be interpreted as an energy density distribution over the (a,b) time-scale plane. The energy of a signal is mainly concentrated on the time-scale plane around the ridges of the wavelet transform [13]. These locations where the frequency of the scaled wavelet coincides with the local frequency of the signal are denoted by

$$a_r(b) = \frac{\omega_0}{\phi'(b)} = \frac{2\pi f_0}{f_i(b)} \tag{14}$$

where $\phi'(b)$ implies the derivative of the phase and ω_0 (or f_0) is the central frequency of the parent wavelet, i.e. the frequency on which the Fourier transform of the parent wavelet focuses. Note that Eq. (14) illustrates that the scales corresponding to the ridges, a_r, can be directly used to identify the instantaneous frequency. The wavelet coefficients along these ridges form the wavelet skeleton.

?1994-2018 China Academic Journal Electronic Publishing House. All rights reserved. http://www.cnki.net

The wavelet transform is a linear representation of a signal. Thus, it follows that for a given N functions x_i and N complex values α_i $(i = 1, 2, \cdots, N)$

$$(W_g \sum_{i=1}^{N} \alpha_i x_i)(a, b) = \sum_{i=1}^{N} \alpha_i (W_g x_i)(a, b) \tag{15}$$

This property is convenient for the analysis of multi-component signals.

In the simplest structural identification problem of free vibration or impulse response, the system has a distinguishable enveloped sinusoidal behavior given by

$$h(t) = A_0 e^{-\xi\omega_n t} \cos(\omega_n \sqrt{1 - \xi^2} t) = A_0 e^{-\xi\omega_n t} \cos(\omega_D t) \tag{16}$$

where A_0 is the initial displacement condition, and θ represents the phase shift. The analytical signal is then

$$z(t) = A_0 e^{-\xi\omega_n t + i\omega_D t} \tag{17}$$

The amplitude function is given by

$$A(t) = |z(t)| = A_0 e^{-\xi\omega_n t} \tag{18}$$

with phase described by

$$\phi(t) = \angle z(t) = \omega_D t \tag{19}$$

Thus, the damped natural frequency can be determined from the derivative of the phase. Assuming a lightly damped system, where $\omega_D \approx \omega_n$, the damping can be determined from Eq. (18).

3.2. Edge effect theory

Despite the good results obtained with the CWT, the edge effect was found to be cumbersome for relatively short signals. For the Morlet wavelet, the use of a Gaussian window on the Fourier basis functions makes the precise definition of temporal duration impractical. The time and frequency resolutions of the Morlet wavelet are given by

$$\Delta t_i = \frac{1}{\sqrt{2}} \frac{f_0}{f_i} \tag{20}$$

and

$$\Delta f = \frac{f_i}{2\pi\sqrt{2} f_0} \tag{21}$$

As for large-scale civil engineering structures, such as skyscrapers, long-span suspension and cable-stayed bridges, high industrial chimneys and TV-towers, the frequencies are low. From Eq. (20), it can be seen that the time windows of the wavelet needs to be elongated at these regions. At both ends of the signal less than Δt_i, the part wavelet function outside the signal makes the incomplete wavelet transform, i.e. the edge effects. Thus, the resultant wavelet coefficients in these regions have questionable accuracy, and are very disadvantageous for signal reconstruction. The edge effect has been studied in a variety of research areas, such as in weather analysis [14], geodesy [15], and mechanics [16]. The cone-of-influence [17], also known as the radius-of-trust (time-width of the edge-effect), was already qualitatively characterized [18]. Kijewski and Kareem [17] used a simple padding scheme to meliorate the edge-effect. Padding is one of the simplest methods of meliorating the edge-effect. There are also other methods for reducing the edge-effect: zero padding, value padding, decay padding, repeating the signal and reflecting the signal [19]. However, these classical methods cannot ensure the continuity of the phase, and its feature on the edge is in doubt.

3.3. Edge effect melioration: prediction extension

Here, a novel method that adopts the auto-regressive moving average (ARMA) model to extend the time series beyond the actual time span is presented (see Fig. 2). In fact, this procedure predicts the values of the time series beyond both ends based on the existing information, which need not add any spurious information on the original time series. The extended region, being an extension of the actual signal in that location, preserves the locale spectral contents, permitting the end effects to consume the surrogate values while leaving the actual signal undamaged. The wavelet coefficients obtained from these augmentations can then simply be neglected in the analysis, and the true signal is maximally analyzed by the wavelet. Compared with formal methods, the approach has good continuity at both ends of the signal and preserves the frequency and bandwidth characteristics of the signal.

If a data set with time series can be fit into an ARMA model, it can be described as follows:

$$x_t - \phi_1 x_{t-1} - \cdots - \phi_p x_{t-p} = a_t - \theta_1 a_{t-1} - \cdots - \theta_q a_{t-q} \tag{22}$$

where p and q are the orders of the AR and MA operator, ϕ_i $(i = 1, 2, \cdots, p)$ and θ_j $(j = 1, 2, \cdots, q)$ denote the coefficients of the AR and MA operator, respectively, and a_t means the white noise sequence.

In Eq. (22), there are $(p + q + 1)$ unknown parameters, $\phi_1, \phi_2, \cdots, \phi_p$, $\theta_1, \theta_2, \cdots, \theta_q$ and a_t. Here, the least square

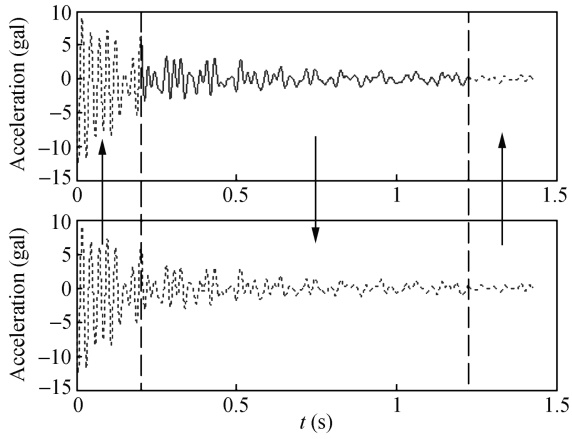

Fig. 2. Schematic demonstration of the prediction extension based on the ARMA model.

?1994-2018 China Academic Journal Electronic Publishing House. All rights reserved. http://www.cnki.net

method is used to estimate the values. The orders of model could be calculated by the mathematical statistics method or information criterion. And A-information criterion (AIC) is adopted since it considers the degree of closeness between the fitted model and original data. In addition, it takes into account the number of undetermined parameters in the model. Hence, it is the best model when the criterion function reaches an extremely small one.

Then, the formula of prediction can be obtained according to the model formula, where $\hat{x}_t(L)$ is the future L step value after the time t, $\hat{x}_t(i) = x_{t+i}$ $(i \le 0)$, then

$$\hat{x}_t(L) = \begin{cases} \sum_{i=1}^{p} \varphi_i \hat{x}_i(L-i) - \sum_{j=0}^{q-L} \theta_{L+j} a_{t-j}, & L \le q \\ \sum_{i=1}^{p} \varphi_i \hat{x}_t(L-i), & L > q \end{cases} \tag{23}$$

4. A numerical example

To better understand the sensitivity of the methods to various kinds of problems, the American Society of Civil Engineers (ASCE) developed a benchmark model [20]. The structure shown in Fig. 3 is a four-storey, two-bay by two-bay steel frame scale model in the Earthquake Engineering Research Laboratory at the University of British Columbia (UBC). It has a dimension of 2.5 m × 2.5 m in plan and 3.6 m in height. The columns and floor beams are modeled as the Euler–Bernoulli beams in both finite element models. The braces are bars with no bending stiffness. It is a 12-DOF shear-building model that constrains all degrees except two horizontal translations and one rotation per floor. The finite element models, by removing the stiffness of various elements, can simulate damage to the structure. Fig. 4 illustrates node numbering in the finite element model. The excitations are applied to each floor,

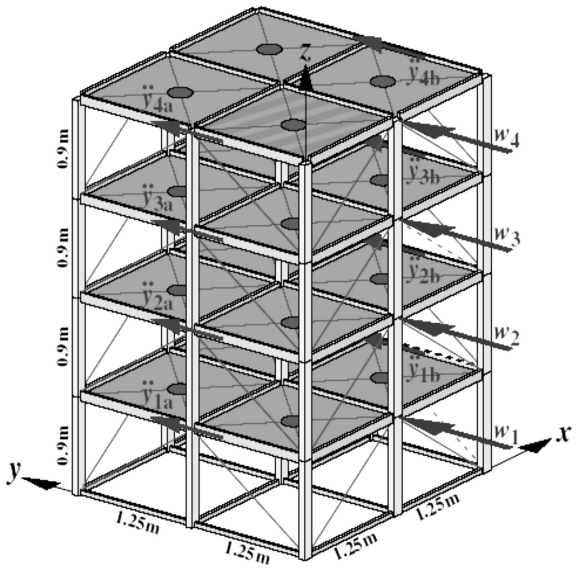

Fig. 3. Schematic drawing of the benchmark model.

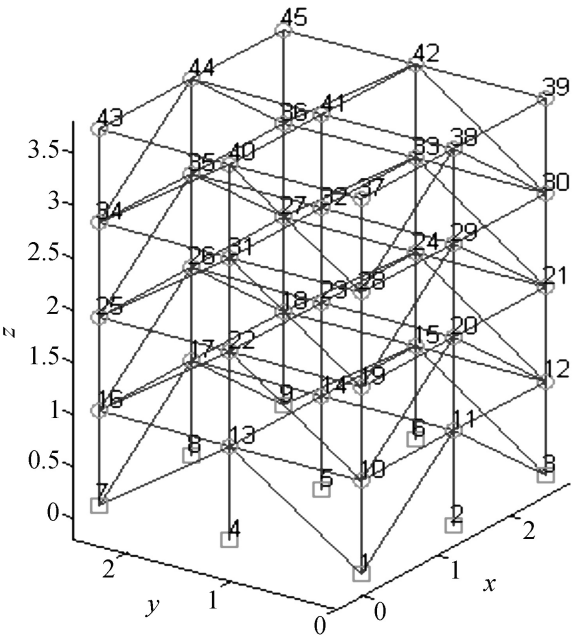

Fig. 4. Node and element numbering in the FE model.

which are modeled as the filtered Gaussian white noise processes passing through the sixth-order low-pass Butterworth filter with a 100 Hz cutoff, and the sampling frequency is 1000 Hz. The response of the structure in the Y direction at node 41 is selected, and then the structural free vibration response can be obtained by the random decrement technique (RDT) [21], as shown in Fig. 5(b).

The resultant scalogram and wavelet ridge are provided in Fig. 6, in which the ridges are straight lines because the simulated system is a linear system. Note that both the scalogram and the wavelet ridge isolate the involved frequency bands, but more precisely in the form of ridges. Fig. 7(a) manifests a rounded hump, very evident in the three modes; and the end effects at low frequencies leave little useable signal for a reliable system identification. The pre-

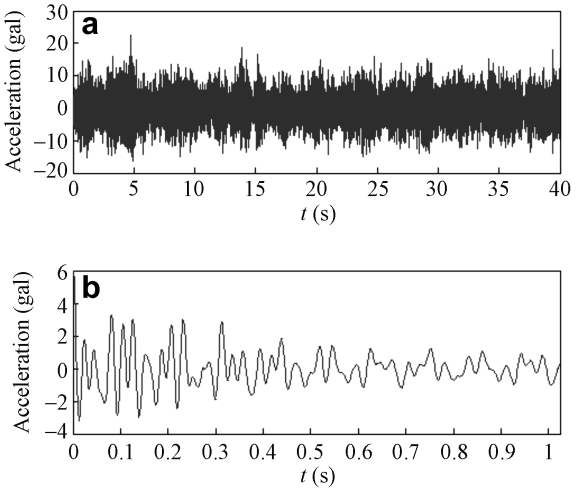

Fig. 5. Simulated acceleration result of node 41 and its RDT signal.

?1994-2018 China Academic Journal Electronic Publishing House. All rights reserved. http://www.cnki.net

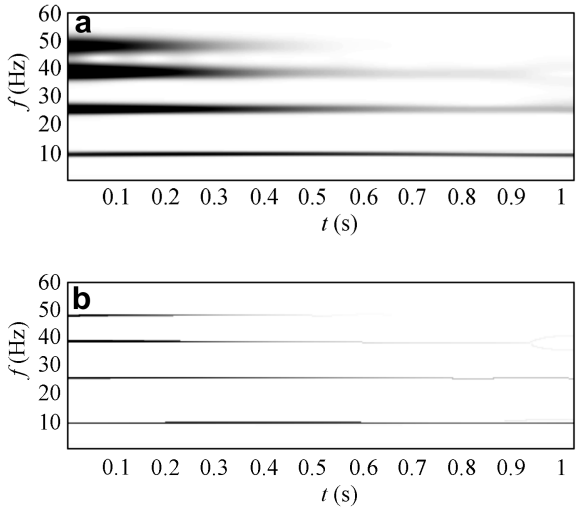

Fig. 6. Wavelet scalogram and wavelet ridge.

diction extension method is used in Fig. 7(b), revealing the marked improvement in the initial region of the signal. The damping may be identified through a linear fitting to the natural log of the wavelet amplitude along the ridges separately. In the case of a nonlinear system, a piecewise analysis is necessary to capture time-varying dynamic properties. The identified results are listed in Table 1.

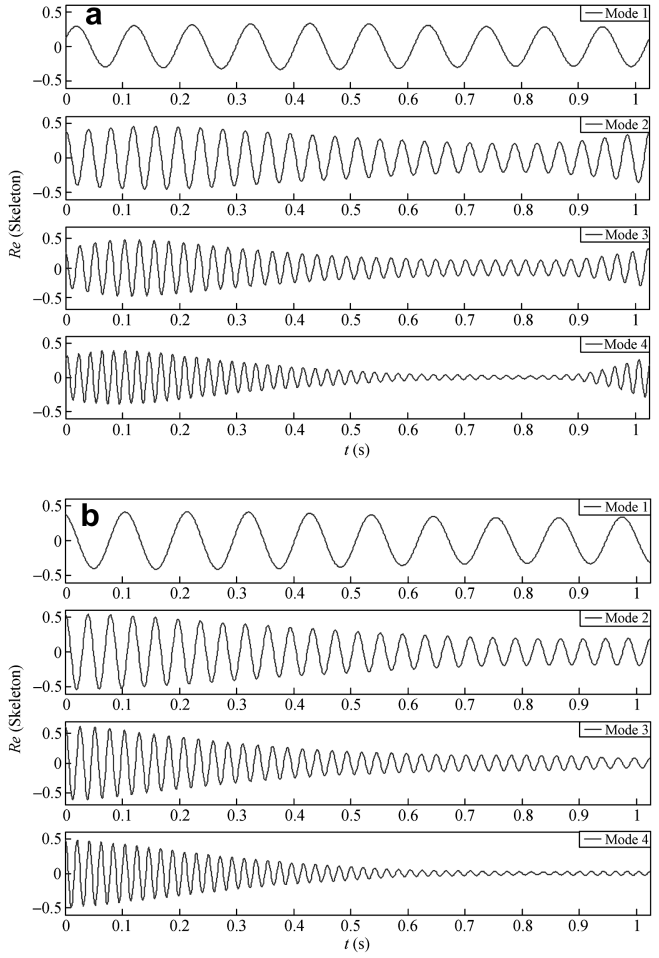

Fig. 7. Real component of the wavelet skeleton. (a) Original results; (b) treated results.

Table 1
Results of parameter diagnosis from the benchmark model.

	Frequency (Hz)		Error (%)	Damping ratio		Error (%)
	ASCE	Wavelet		ASCE	Wavelet	
First mode	9.41	9.2586	1.609	0.01	0.0101	1
Second mode	25.60	25.4085	0.748	0.01	0.0100	0
Third mode	38.85	38.4877	0.933	0.01	0.0105	5
Fourth mode	48.37	48.0098	0.745	0.01	0.0103	3

5. Shaking table test and data analysis

From the results discussed above, it can be easily seen that the two main features make the CWT particularly attractive for the diagnosis of special events in structural behavior during an earthquake excitation. Firstly, the vibration modes can be automatically decoupled in most cases where the natural frequencies are not too close, allowing for an accurate extraction of the instantaneous frequencies and damping parameters. Secondly, essential information is contained in a small subset of the CWT, namely in the maxima lines and ridges. Any changes in frequency content, e.g. the initiation of stiffness degradation, sudden occurrence of a non-ductile event, energy exchange between modes through response coupling, or pounding between structural components can be identified by the scalogram. Here, the relation between the dynamic properties of structures and energy accumulation and its change rates is studied by a scale model of a three-storey reinforced concrete (RC) frame-share wall structure.

5.1. Energy principles

From the Wavelet transform, the scalogram of energy distribution may be generated by the squaring modulus of the transform. This representation, analogous to the spectrogram, represents the energy content of the signal at distinct time and frequency (scale) pairs; while the energy distribution in the scalogram is a multi-resolution:

$$SG(a,b) = |W(a,b)|^2 \tag{24}$$

The mean wavelet spectrum can be estimated by the integration over the time variable as discussed in Ref. [22], which may be expressed as follows for a signal with finite duration T:

$$S_{wt}(a) = \frac{2}{C_g}\left[\frac{1}{T}\int_0^T SG(a,b)\mathrm{d}b\right] \tag{25}$$

The energy accumulations in the frequency domain, denoted by $E(f)$, are determined by an integral operation at each frequency of the mean wavelet spectrum through the following expression:

?1994-2018 China Academic Journal Electronic Publishing House. All rights reserved. http://www.cnki.net

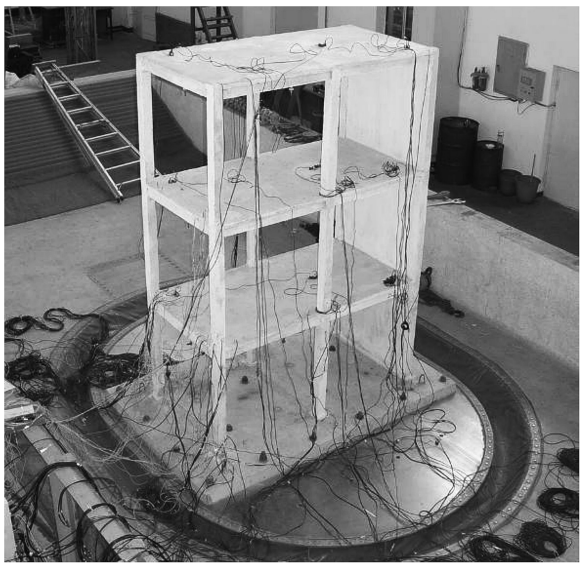

Fig. 8. Experimental setup for shaking table tests.

$$E(f_i) = \int_{f_1}^{f_i} S_{WT}(f_0/f)\mathrm{d}f \quad \text{for} \quad i = 1, 2, \cdots n \tag{26}$$

Similarly, a time analog to the mean wavelet spectrum may be defined by

$$S_{WT}(b) = -\int_{f_1}^{f_n} SG(f_0/f, b)\mathrm{d}f \tag{27}$$

Energy accumulations in the time domain, denoted by $E(t)$, are then appropriately determined by

$$E(b_j) = \int_{b_1}^{b_j} S_{WT}(t)\mathrm{d}b \quad \text{for} \quad j = 1, 2, \cdots m \tag{28}$$

Each change rate of these accumulation measures with respect to frequency or time is denoted by, respectively, $\mathrm{d}E(f)/\mathrm{d}f$ or $\mathrm{d}E(t)/\mathrm{d}t$, and the maximum values of these accumulation rates will be of particular interest in subsequent discussions as they identify the arrival of significant events in the time and frequency domains.

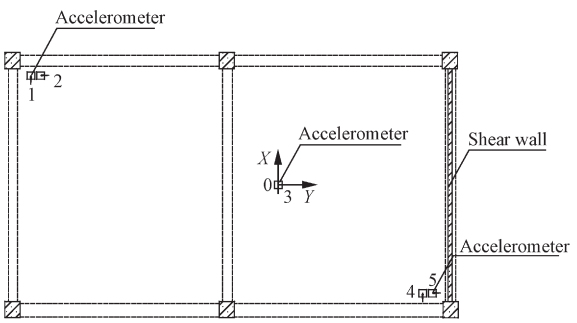

Fig. 9. Schematic of the location of accelerators.

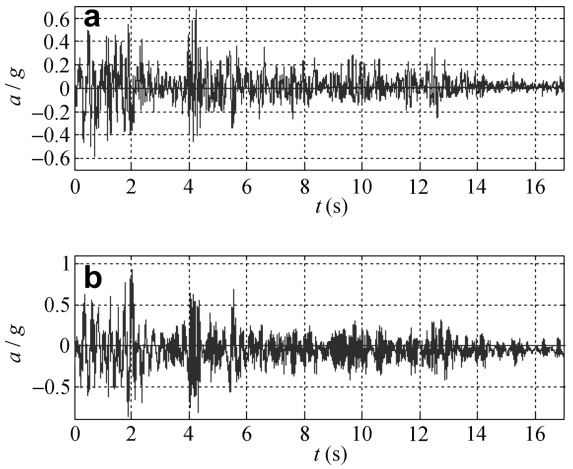

Fig. 10. The acceleration records form the base (a) and the third storey (b) of the building.

5.2. Model design

The experiment was carried out with the earthquake simulator facility in the State Key Laboratory of Coastal and Offshore Engineering, Dalian University of Technology, China. The facility includes a 4 m × 3 m steel platform, driven by servo-hydraulic actuators and an MTS analog electronic control system, which makes fine feedback over accelerations, velocities and displacements. With a maximum horizontal and vertical displacement of ±75 mm and 50 mm, respectively, the shaking table has about ten tons of payload capacity and a frequency range from 0.1 Hz to 50 Hz [23].

The tests model the scale of a three-storeyed building with the RC frame-share walls under simulated seismic excitations, as shown in Fig. 8. The member dimensions and detailed structural characteristics of the testing model can be obtained from Ref. [24]. The data were acquired simultaneously at the rate of 500 Hz from 16 channels. Accelerometers and load cells were used to measure the

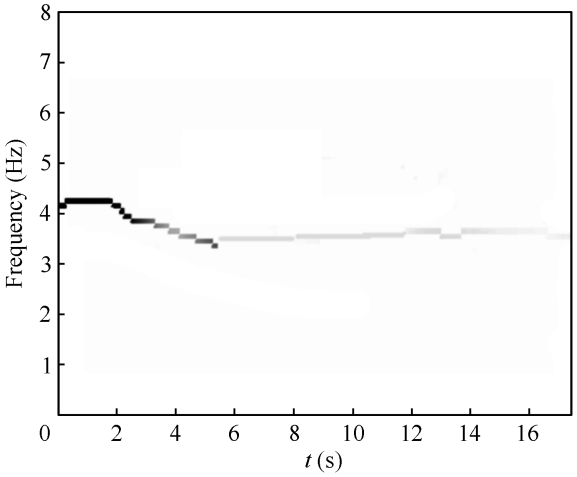

Fig. 11. Instantaneous frequency identified from wavelet transform.

?1994-2018 China Academic Journal Electronic Publishing House. All rights reserved. http://www.cnki.net

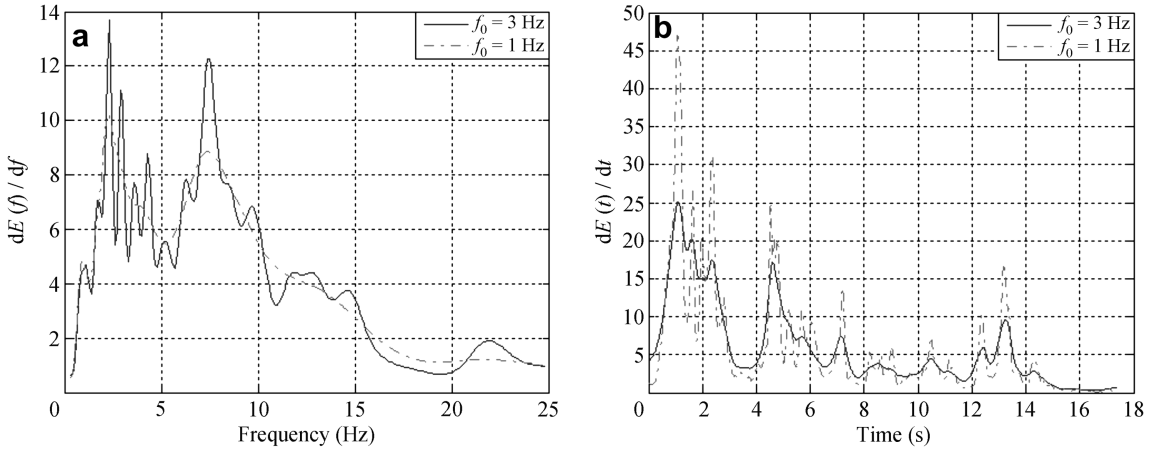

Fig. 12. Change of energy accumulation in frequency (a) and time domain (b).

acceleration at each storey, and shear forces on the columns of the first storey. Fig. 9 shows the accelerator placement on each floor of the building model.

5.3. Results of earthquake simulation tests and interpretation

The base excitations were the El Centro earthquake NS acceleration time series in 1940 and were scaled with the increasing peak ground acceleration (PGA) being 0.2 g, 0.3 g, 0.5 g, 0.6 g, 0.8 g and 1.0 g. The tested structure was excited by the six consecutive horizontal acceleration processes with increasing intensities on the shaking table, without repairing or strengthening during the acceleration processes. The records with 0.3 g PGA from the base and response of the third storey of the tested structure in the X direction at location 3 (center of mass) are shown in Fig. 10. Since the global response is mainly captured by the lower frequency while the higher frequency tends to capture the local response of the structure, the instantaneous fundamental frequency was determined by the wavelet method that was introduced previously. It can be observed that the instantaneous natural frequencies identified are constant for the first 2 s, then slowly decrease as a result of the stiffness degradation, and again constant over the last 6 s (Fig. 11).

The energy accumulation and its change rates in frequency and time domain shown, respectively, in Figs. 12 and 13, offer a complete description of the energetic components of the quake. Due to the short duration of the earthquake process, a Morlet wavelet with central frequency of $f_0 = 1$ Hz was first applied, and a more detailed examination of the frequency content was performed by using $f_0 = 3$ Hz to study the energy accumulation process. From the change rate of the energy accumulation in the frequency domain as shown in Fig. 12, it is evident that the maximum change rate in the signal is constrained between 2.0–3.1 Hz and 6.9–8.0 Hz. There is little change in the energy accumulation within the signal beyond 16 Hz. In the time domain, it is evident from Fig. 12 that the analysis with $f_0 = 1$ Hz is superior in capturing many of the individual pulses in the record to the one with $f_0 = 3$ Hz, though both the analyses capture the same overall trends. The analysis with $f_0 = 1$ Hz indicates that most rapid changes of the energy within the signal occur between

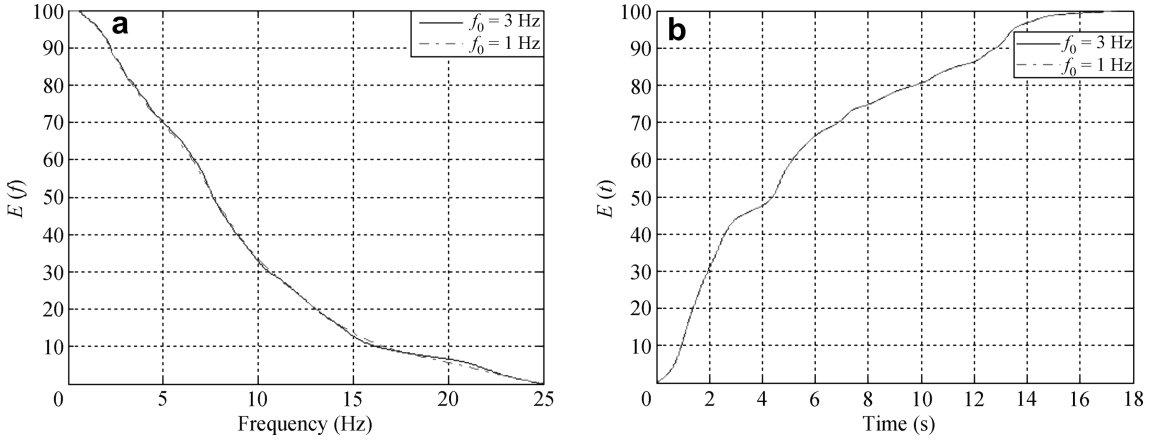

Fig. 13. Energy accumulation in frequency (a) and time domain (b).

?1994-2018 China Academic Journal Electronic Publishing House. All rights reserved. http://www.cnki.net

0.5 s and 3 s. In the time domain, the occurrence time of three distinct events is discernable: 1.0 s, 4.5 s and 13.2 s, with the most rapid change in energy being associated with the first in the series. The energy falls off very quickly following this flurry.

The curve of energy accumulation in the time domain is not smooth with many small pulses due to the arrival of the P and S waves. With the arrival of the first pulse at 1.0 s, the energy is accumulated from 11% to 44%. The intermediate event at 4.5 s brings the energy level up to 66%, with the next major event at 13.2 s, causing a jump in accumulated energy from 90% to 97%. The accumulated energy shows a gentle trend to slowly level off near 3.5 s at about 45% of the total signal energy. The minor event at 7.0 s brings the accumulated energy to 71%, followed by the event near 13.2 s at which the accumulated energy has reached 97% and has been steadily ascending. The accumulation of energy in the frequency domain shows that the dominant influx of energy comes from the signals with frequencies between 2.0 Hz and 5.0 Hz. At the time, the signal energy jumps from 70% to 95%. Signals with frequencies below 1 Hz almost have no contribution to the energy.

Comparing the energy accumulation with the change of frequencies of the structure in Fig. 13, it can be seen that there is an obvious delay between the frequency degradation and the energy accumulation and its change rate. The signal frequency degradation mainly occurs between 2 s and 6 s, with a stationary trend from 2.4 s to 2.9 s; while the energy accumulation and its change rate, as mentioned above, mainly occur between 0.6 s and 4.5 s, with a stationary trend from 3.5 s to 4.2 s. There is about 1.1–1.5 s delay between them. Although the results indicate that each of these earthquake records and their associated time and frequency characteristics depend strongly on local soil conditions, and that topography should not be considered to be representative of the complete ground motions, these results still highlight the wavelet's ability to uncover the intermittent and nonlinear characteristics of the process.

6. Concluding remarks

Up to now, the wavelet transform has scarcely been applied to structural health monitoring in civil engineering. This study applied a wavelet approach for the detection and assessment of progressive damage in the structural system, and a novel method called "prediction extension" to remedy the problem of edge effect is presented, which has been validated using the vibration response obtained by numerical simulation for the ASCE benchmark. The instantaneous modal parameters for the four vibration modes are identified, and their values are compared to the official data. The results have shown that they are in good agreement. And the relation between the dynamic properties of structure and energy accumulation and its change rates is also discussed through a shaking table experiment.

The investigations in this paper have validated that the wavelet method is a promising and powerful analytical tool to identify the dynamical feature of the input and output in both time and frequency domains.

Acknowledgements

This work was jointly supported by the Program for Changjiang Scholars and Innovative Research Team in University (No. IRT0518), the 111 Project (No. B08014), Natural Science Foundation of China (No. 50708013), the Research Fund for the Doctoral Program of Higher Education (No. 20070141036), the China Postdoctoral Science Foundation Project (No. 20070420113) and the Open Fund of Liaoning Province Key Laboratory of Structural Engineering, Shenyang Jian Zhu University (No. JG200718).

References

[1] Alphose Z. Structural health monitoring, damage detection and long-term performance. Eng Struct 2005;27(12):1713–4.
[2] PIANC. Seismic design guidelines for port structures. The Netherlands: AA Balkema Publishers; 2001.
[3] Dong YF, Li YM, Xiao MK, et al. Analysis of earthquake ground motions using an improved Hilbert–Huang transform. Soil Dyn Earthquake Eng 2008(28):7–19.
[4] Apostolou M, Gazetas G, Garini E. Seismic response of slender rigid structures with foundation uplifting. Soil Dyn Earthquake Eng 2007;27(7):642–54.
[5] Hancock J, Bommer JJ. Using spectral matched records to explore the influence of strong-motion duration on inelastic structural response. Soil Dyn Earthquake Eng 2007;27(4):291–9.
[6] Hamzehloo H. Strong ground motion modelling of causative fault for the 2002 Avaj earthquake, Iran. Tectonophysics 2005;409(1–4):159–174.
[7] Iyamas J, Kuwamura H. Application of wavelets to analysis and simulation of earthquake motion. Earthquake Eng Struct Dyn 1999;28:255–72.
[8] Feldman M, Braun S. Identification of nonlinear system parameters via the instantaneous frequency: application of the Hilbert transform and Winger-Ville techniques. In: Proceedings of 13th IMAC, Nashville, Tennessee, 1995, p. 637–42.
[9] Frederik JS, Ben DED, Richard MA. Automatic detection and rapid determination of earthquake magnitude by wavelet multiscale analysis. Earth Planet Sci Lett 2006;250(1–2):214–23.
[10] Chui CK. Wavelet analysis and applications: An introduction to wavelet. San Diego: Academic Press; 1992.
[11] Daubechies I. Ten lectures on wavelet. Montpellier: Capital City Press; 1992.
[12] Telesca L, Lapenna V, Alexis N. Multiresolution wavelet analysis of earthquakes. Chaos Solitons Fractals 2004;23(2):741–8.
[13] Huang CS, Su WC. Identification of modal parameters of a time invariant linear system by continuous wavelet transformation. Mech Syst Signal Process 2007;21(4):1642–64.
[14] Torrence C, Compo G. A practical guide to wavelet analysis. Bull Am Meteorol Soc 1998;79(1):61–78.
[15] Zheng D, Chao B, Zhou Y, et al. Improvement of edge effect of the wavelet time-frequency spectrum: application to the length-of-day series. J Geodesy 2000;256(74):249–54.
[16] Ruzzene M, Fasana A, Garibaldi L, et al. Natural frequencies and damping identification using wavelet transform: application to real data. Mech Syst Signal Process 1997;11(2):207–18.

?1994-2018 China Academic Journal Electronic Publishing House. All rights reserved. http://www.cnki.net

[17] Kijewski T, Kareem A. On the presence of end effects and their melioration in wavelet-based analysis. J Sound Vibration 2002;256(5):980–8.
[18] Simonovski I, Boltemar M. The norms and variances of the Gabor, Morlet and general harmonic wavelet functions. J Sound Vib 2003;264(3):545–57.
[19] Addison P. The illustrated wavelet transform handbook: Introductory theory and applications in science, engineering, medicine and finance. London: Institute of Physics Press; 2002.
[20] Johnson EA, Lam HF, Katafygiotis L, et al. A benchmark problem for structural health monitoring and damage detection. In: Proceedings of the 14th ASCE engineering mechanics conference, Austin, TX, 2000.
[21] Rodrigues J. Stochastic modal identification: methods and applications in civil engineering structures (Ph.D. Thesis). University of Porto (FEUP/LNEC), 2004.
[22] Lewalle J. Applications of continuous wavelets to data analysis, Part I: Wavelets without lemmas. In: Von Karman Institute for Fluid Dynamics, Lecture Series. Advanced Measurement Techniques, April, 1998.
[23] Li HN. Profile school of civil and hydraulic engineering, Dalian University of Technology. Adv Struct Eng 2004;7(1):111–2.
[24] Yi TH, Li HN, Li B, et al. Seismic response analysis using wavelet spectrum and structural damage assessment. J Vib Shock 2006;25(5):32–6, [in Chinese].

?1994-2018 China Academic Journal Electronic Publishing House. All rights reserved. http://www.cnki.net